



**Full Length Article**

## Comparative Transcriptome Analysis of Winter Wheat under Different Levels of Shading

Xiaorong Li<sup>1†</sup>, Jianfeng Li<sup>1,2†</sup>, Hongzhi Zhang<sup>1,2</sup>, Lihong Wang<sup>1,2</sup>, Zhong Wang<sup>1,2</sup>, Yueqiang Zhang<sup>1,2</sup>, Zheru Fan<sup>1,2</sup>, Jia Shi<sup>1,2</sup> and Qi Zhao<sup>1,2\*</sup>

<sup>1</sup>Institute of Nuclear and Biological Technology, Xinjiang Academy of Agricultural Sciences, Urumqi 830091, China

<sup>2</sup>Key Laboratory of Crop Ecophysiology and Farming System in Desert Oasis Region, Ministry of Agriculture, P.R. China, Urumqi 830091, China

\*For correspondence: zhq0817@sina.com

†Contributed equally to this work and are co-first authors

Received 18 February 2020; Accepted 12 March 2020; Published 31 May 2020

### Abstract

Wheat-based intercropping systems are widely applied by farmers to improve the land equivalent ratio. However, intercropping leads to shading of wheat and the grain yield might be decreased due to reduced photosynthetic rate and leaf area index. This study was conducted to investigate the changes on transcriptional profile of wheat leaves in response to different levels of shading. Winter wheat (*Triticum aestivum* L. 'Xindong 20') was planted under three shading levels, namely, no-shading (control), 25% shading, and 75% shading. The dry weight of wheat plants was determined at flowering and maturity periods. The photosynthetic rate of flag leaves was determined at flowering and filling stages. Flag leaves from each group were collected at the heading stage for RNA sequencing. Quantitative reverse transcription-polymerase chain reaction (qRT-PCR) was used to validate the results of RNA sequencing. Wheat plants had longer growth period, decreased dry weight and photosynthetic rate of flag leaves under different levels of shading. A total of 12,597 and 28,349 differentially expressed genes (DEGs) were identified in 25% shading group and 75% shading group, respectively. Functional enrichment analyses suggested that upregulated genes in 25% shading group were mainly involved in regulating cell homeostasis, especially in redox homeostasis. The upregulated genes in the 75% shading group were involved in nitrogen compound metabolic process. In addition, the downregulated genes of the two groups were both enriched in phosphorus metabolic processes. A total of 2,015 unigenes were identified as transcription factors. Ten of 16 DEGs (*At3g21620*, *ETR1*, *1-SST*, *PSB28*, *HEMH*, *Os10g0493600*, *6-FEH*, *CIN2*, *PORA*, and *CPX*) involved in porphyrin and chlorophyll metabolism, photosynthesis, and galactose metabolism were successfully validated by qRT-PCR. In conclusion, these data, revealed transcriptional dynamics of wheat under different shading levels, will provide essential clues for deciphering the gene regulatory networks mediating the wheat response to shading, especially at heading stage. © 2020 Friends Science Publishers

**Keywords:** Low light stress; Homeostasis; ROS; Shading; Transcriptome; Wheat

### Introduction

Wheat (*Triticum aestivum* L.) is widely planted worldwide including arid and semi-arid regions and is one of the most important food crops (Cossani and Reynolds 2012; Gao *et al.* 2019). In China, wheat is the second most widely grown crop after rice (Li *et al.* 2017). With an increase in human population, it is estimated that crop production will be doubled by 2050 to meet the food demand (Li *et al.* 2017). Therefore, efforts are still needed to increase wheat yield.

Xinjiang Uygur Autonomous Region, located in Northwest China, is an important wheat-producing region. Fruit tree-based intercropping systems are widely applied by local farmers because that this cultivation method can prevent soil erosion, decrease water loss, enhance carbon

sequestration, organic carbon, soil nutrient status, and nutrient cycling (Bergeron *et al.* 2011; Rivest *et al.* 2009; 2013). Moreover, this method significantly increases the land equivalent ratio (Yu *et al.* 2015).

Photosynthesis and nitrogen fertilizer are two major factors that affect plant production. More than 90% of grain yield depends on photosynthesis (Makino 2011). During photosynthesis, photosynthetic pigments absorb light energy and convert it into chemical energy in the form of carbohydrates, which are needed for plant growth (Wu *et al.* 2018). The photosynthetic rate is mainly determined by three aspects, namely, light intensity, temperature and carbon dioxide concentration. Among these factors, the light intensity is of great importance. Generally, higher light intensity corresponds to higher photosynthetic rate. The

competition for light between wheat plants and intercropping fruit trees, which lead to shading to wheat plants, might decrease photosynthetic rate and leaf area index in wheat leaves, thus decrease the grain yield of wheat (Kemp and Whingwiri 1980; Mu *et al.* 2010). For example, apricot-, walnut-, and jujube-based intercropping systems lead to a decrease of 31.9, 36.2 and 11.3%, respectively in the photosynthetic rate of wheat, compared to monocultured wheat (Qiao *et al.* 2019). Shade-grown plant show a degree of etiolation, which is as another cause of reduced growth and yield of crop plants (Batool *et al.* 2020).

Winter wheat is the second most planted crop in China after rice. Fruit tree-based intercropping systems are widely favored in several areas of China. However, the productivity of intercropping crops in many agroforestry systems can be significantly decreased because of the shading effect from neighboring tree. Many individual components and pathways operating during plants adaptation to low light stress have been identified, however the molecular mechanism(s) on the wheat response to shading are still not well known. There are opposing findings that shading can increase the leaf area index and photosynthetic rates and delay leaf senescence and therefore, increase the wheat grain yield (Li *et al.* 2010; Xu *et al.* 2016). Whether shading increases or decreases the wheat yield depends on the level of shading (Wang *et al.* 2003; Guo *et al.* 2014; Li *et al.* 2017). However, the molecular mechanisms in response to different levels of shading in wheat leaves are not well understood.

In this study, an RNA sequencing (RNA-seq) analysis on wheat flag leaves at heading stage under different shading conditions (*i.e.*, no shading, and 25 and 75% shading treatments) was performed. Through a comparative analysis, we surveyed transcriptome changes in wheat leaves in response to different levels of shading conditions. As a result, we find some possible genes, which participated in shading response in wheat leaves, and revealed the possible regulatory mechanism in wheat leaves in response to different level of shading on transcriptional level.

## Materials and Methods

### Experimental site

The winter wheat (*Triticum aestivum* L. 'Xindong 20') individuals were planted at zepu base (E 77°16', N 38°10', altitude 1266 m) in Kashi, Xinjiang, China between 2016 and 2017.

### Plant materials and experimental design

We established three treatment groups: the control (sample name: TDC0), 25% shading group (sample name: TDT1), and 75% shading group (TDT3). The individuals in the control were grown under natural light. In 25% shading group, they were shaded by 10% shading was provided at

the elongation stage and 25% at the heading stage. In 75% shading group, they were shaded by 30% shading was done at the elongation stage and 75% at the heading stage. For shading treatments, individuals were covered by black nylon mesh with different luminous transmittance. The shade mesh was kept at about 100 cm above the wheat canopy and was adjusted depending on the plant growth to ensure enough ventilation. Each shading treatment included three repeated plots and each plot covered 8 m<sup>2</sup> (4 m × 2 m).

Before planting, 150 kg/hm<sup>2</sup> urea and 375 kg/hm<sup>2</sup> diammonium phosphate were applied as base fertilizers. Then, 150 kg/hm<sup>2</sup> urea and 300 kg/hm<sup>2</sup> urea were applied at the returning stage and jointing stage, respectively. The sowing amount of winter wheat was 270 kg/hm<sup>2</sup>, and the row spacing was 20 cm. Drip irrigation was carried out 5 times during the whole season (*i.e.*, at wintering stage, returning stage, elongation stage, flowering stage, and grain filling stage). All other cultivation measures were consistent among groups.

### Sampling and measurement

The dry weight of wheat plants was determined at the flowering period and maturity period. The photosynthetic rate of flag leaves was determined at flowering and filling stages using Li-6400 portable photosynthetic system (Li-Cor, Lincoln, NE, USA) as described previously (Li *et al.* 2017). Briefly, flag leaves with uniform fertility progress and uniform illumination on healthy plants were selected, and the photosynthetic rate was determined between 9 am and 12 noon on a sunny day. The artificial light intensity was set as 1200  $\mu\text{mol}\cdot\text{m}^{-2}\cdot\text{s}^{-1}$ . At heading stage, samples were collected after three days of complete shading treatment. Similar-sized ten pieces of flag leaves were collected from each plot and were mixed as one sample for RNA extraction.

### Construction of complementary DNA (cDNA) library and RNA-sequencing

Total RNA of the flag leaves was extracted using TRIzol reagent (ThermoFisher, Waltham, MA, USA). RNA degradation and purity were checked using 1% agarose gels and spectrophotometer (IMPLEN, CA, USA), respectively. RNA concentration and integrity were assessed with commercial kits, respectively. Then, RNA sequencing libraries were generated using 1  $\mu\text{g}$  RNA from each sample. Qualified cDNA libraries were submitted for Illumina HiSeq platform to perform RNA sequencing.

### Data analysis

Raw reads in FASTQ format were quality-controlled by in-house Perl scripts to obtain clean reads. During this step, reads containing adapter, ploy-N (>10%), and with low quality ( $Q_{\text{phred}} \leq 20$  in more than 50% bases) were removed.

Q20, Q30 and guanine-cytosine (GC) content were calculated. The clean reads were then aligned to the wheat reference genome using HISAT version 2.1.0 (Kim *et al.* 2015) with default parameters. Gene expression was estimated as fragments per kilobase per million (FPKM) base pairs sequenced, which is the most frequently used method in estimating gene expression levels (Trapnell *et al.* 2010), using HTSeq (version 0.6.1) with default parameter of -m union (Anders *et al.* 2015). Generally, the gene expression with FPKM greater than 0.1 is regarded as a threshold to determine whether a gene is expressed or not. Correlations between RNA-sequencing data of each sample were calculated by the Pearson's correlation coefficient in R software (version 3.4.2, Free Software Foundation, Boston, USA). Qualified RNA-sequencing data of samples in each group should meet the requirement of  $r^2$  greater than 0.8.

Differential expression analyses were performed using the "DESeq2" package of R (Love *et al.* 2014). To reduce the false discovery rate,  $P$ -values were adjusted by Benjamini and Hochberg (1995) approach. The genes fulfilling the thresholds of adjusted  $P$ -value  $< 0.05$  and  $\log_2$  fold change (FC)  $\geq 1$  were regarded as differentially expressed genes (DEGs). Venn diagram was drawn to show overlapped DEGs between each comparison group, and hierarchical clustering was performed using the "Heatmap" package of R to compare expression patterns of the DEGs in each group.

Gene Ontology (GO) database provides gene descriptions and their products, which is applicable to various species. It classifies functions along three aspects: biological process (BP), cellular component (CC), and molecular function (MF) (Ashburner *et al.* 2000; Carbon *et al.* 2017). GO classification of DEGs was performed using Goseq (Young *et al.* 2010) based on hypergeometric distribution.

The DEGs were mapped to Kyoto Encyclopedia of Genes and Genomes (KEGG) pathway database using KOBAS web server (version 2.0) (Mao *et al.* 2005) to examine the dysregulated pathways of DEGs. Corrected  $P$ -value  $< 0.05$  was regarded as a threshold to select the most enriched GO terms and KEGG pathway terms. Transcription factors (TFs) were identified using iTAK software (Zheng *et al.* 2016) with default parameters.

### Validating DEGs with quantitative reverse transcription-polymerase chain reaction (qRT-PCR)

The qRT-PCR was performed to validate RNA sequencing data of 16 DEGs. Total RNA from wheat leaves collected from the three groups was extracted using TRIzol reagent. DNaseI was added to remove genome DNA. The RNA was reverse transcribed into cDNA with a PrimeScript RT reagent kit (Takara, Dalian, China, Code No. RR037A) and purified with QIAquick PCR purification kit (Qiagen). The qRT-PCR was carried out using a light cycler 480 System (Roche) and SYBR GREEN kit (TaKaRa). The qRT-PCR

procedure was as follows: 95°C for 15 min, 40 cycles at 95°C for 10 s, 58°C for 20 s, and 72°C for 20 s. The primers are listed in Table 1. Relative expression of genes was calculated by  $2^{-\Delta\Delta Ct}$  method with tubulin as an internal control (Livak and Schmittgen 2001). Three biological replicates were analyzed and each reaction was performed in triplicate.

## Results

### Comparisons of changes on dry weight and photosynthetic rate under different levels of shading

Under shading conditions, the development of wheat plants was inhibited. Plants have longer growth period (2 days longer in TDT1 and 11 days longer in TDT3, respectively) and decreased leaf size. The dry weight and photosynthetic rate of flag leaves were also determined in each group. The dry weights of plants in 25% shading group and 75% shading group were significantly less than the control group at flowering period ( $P < 0.05$ ). At maturity period, the dry weight of plants in 75% shading group was significantly less than the control group ( $P < 0.05$ ), while there was no significant ( $P > 0.05$ ) difference between 25% shading group and the control (Fig. 1A). Similarly, the photosynthetic rate also showed a continuously decreasing trend among groups. That is, the photosynthetic rates in 25 and 75% shading group were significantly lower than the control group ( $P < 0.05$ ) at flowering period. However, the photosynthetic rate at the grain period was significantly ( $P < 0.05$ ) decreased only in 75% shading group (Fig. 1B).

### RNA sequencing data

A total of 113.07 Gb clean reads were obtained after quality control. Q30 of all samples was larger than 89.65% and GC contents were between 50.63 and 55.54%, indicating high quality of RNA sequencing. Ratios of reads mapped to the reference genome of each sample ranged from 88.34 to 90.6% (Table 2). Pearson correlation analysis showed that the  $r^2$  between pair-wise samples in each group was all larger than 0.9, indicating high repeatability in biological replicates and high reliability of RNA-sequencing data (Fig. 2A).

### Identification of DEGs

Based on the criteria of adjusted  $P$ -value  $< 0.05$  and  $\log_2$ FC  $\geq 1$ , a total of 12,597 DEGs, including 4,466 upregulated genes and 8,131 downregulated genes were identified between TDT1 and TDC0. A total of 28,349 DEGs were identified between TDT3 and TDC0, including 12,371 upregulated genes and 15,978 downregulated genes. A total of 5,532 DEGs were identified between TDT3 and TDT1, including 2,296 upregulated genes and 3,236 downregulated genes (Fig. 2B–D). The total number of DEGs between

**Table 1:** The primer sequence used for qRT-PCR

Gene bank ID	GENE	Sequence (5'-3')	Length(bp)
AA086852	W-CYP98A1-F	CGACTACGGCCCGCACTACATC	179
	W-CYP98A1-R	GTTCCCTCACTACCATTGGCTTTCCTT	
AA0438620	W-PPO-F	GCTGACCGACCTTGACTCCA	104
	W-PPO-R	CCAGGAACAGCAGCGTCT	
AA0153830	W-At3g21620-F	ATGGCTAATCAACTCATCTC	190
	W-At3g21620-R	AAGGTTCAAGACAAAGCCCAA	
AA1246570	W-ACO1-F	ACTTCTTCCTCCACTTGCTCT	101
	W-ACO1-R	ATTTGCATGTATGGCTGTGAGACC	
AA0864380	W-PKL-F	TTAAGTACCACACGGGCAGT	157
	W-PKL-R	CCTGAATCCCTACTCTCGTCA	
AA006795	W-ETR1-F	AGACCGGGAGGCATGTTAGG	166
	W-ETR1-R	GTGATTTGGTGGCGCAGAG	
AA1656990	W-WHAB1.6-F	GCAGCAAGGAGAAGCCAGCATC	214
	W-WHAB1.6-R	GGGAACCCTCGGCGGACAT	
AA0115100	W-Os10g0493600-F	GCTGGAACCCTTCTACTGCG	151
	W-Os10g0493600-R	AAGTTACCCTGGGAATCCCTACTA	
AA0272780	W-6-FEH-F	ATGGCGTATCGCCGTTGCA	198
	W-6-FEH-R	GCGTAGCCAAGTCGCCCCCTC	
AA0318750	W-CIN2-F	GCGTACGTGTACCGGAGCAGGG	153
	W-CIN2-R	GACGACGGCGGACGAGGTGT	
AA1820630	W-1-SST-F	CAAGGACATGGTGAACCTGGCG	127
	W-1-SST-R	GGTGTAGAGCAGGATGACCTGGC	
AA0822510	W-PSB28-F	CGCTGCCCATGTCCATGCG	198
	W-PSB28-R	GACCAAGAATTCCGGCGAACAC	
AA1249400	W-HEMH-F	TCAACCTCTTCGCTGATCC	119
	W-HEMH-R	GGCATAACCCTCTTTACTCT	
AA0275620	W-PORA-F	CTTCAGGGCTAGGTTTAGCAAC	162
	W-PORA-R	CCAAAGACGCCAAGTCCAA	
AA0130320	W-At5g26707-F	AAAAGCCAAATAGAACACTAG	141
	W-At5g26707-R	CTAAATGGGCATTTCATCTC	
AA1616020	W-CPX-F	TTGGACAGCGTGAGGCAGTTT	182
	W-CPX-R	ATCGGAGTTCTTCAAGTCATCAATCAA	
AA086438	W-B-TUBF	GGGCAAGATGAGCACCAA	170
	W-B-TUBR	TCCACGAAGTAGGAGGAGTTCTT	

**Table 2:** The mapped statistics of all samples

Sample name	TDC0_1	TDC0_2	TDC0_3	TDT3_1	TDT3_2	TDT3_3	TDT1_1	TDT1_2	TDT1_3
Total reads	72518502	99514062	72946984	76479352	88167792	92834306	73170976	81721748	96336264
Total mapped	66846096	91920789	66857327	70580568	81864542	87292018	67642629	76507807	88704652
	(92.18%)	(92.37%)	(91.65%)	(92.29%)	(92.85%)	(94.03%)	(92.44%)	(93.62%)	(92.08%)
Multiple mapped	2125572	3411006	1983283	3020043	3121944	3181544	1829799	2824753	3741568
	(2.93%)	(3.43%)	(2.72%)	(3.95%)	(3.54%)	(3.43%)	(2.5%)	(3.46%)	(3.88%)
Uniquely mapped	64720524	88509783	64874044	67560525	78742598	84110474	65812830	73683054	84963084
	(89.25%)	(88.94%)	(88.93%)	(88.34%)	(89.31%)	(90.6%)	(89.94%)	(90.16%)	(88.19%)

TDT3 and TDC0 was 2.25-fold higher than those identified between TDT1 and TDC0. Venn diagram between TDT1 versus TDC0 and TDT3 versus TDC0 showed that there were 2,591 and 18,343 unique DEGs found in TDT1 and TDT3, respectively (Fig. 3A). Another Venn diagram showed that only 1,170 DEGs were continuously differentially expressed in 25 and 75% shading groups (Fig. 3B).

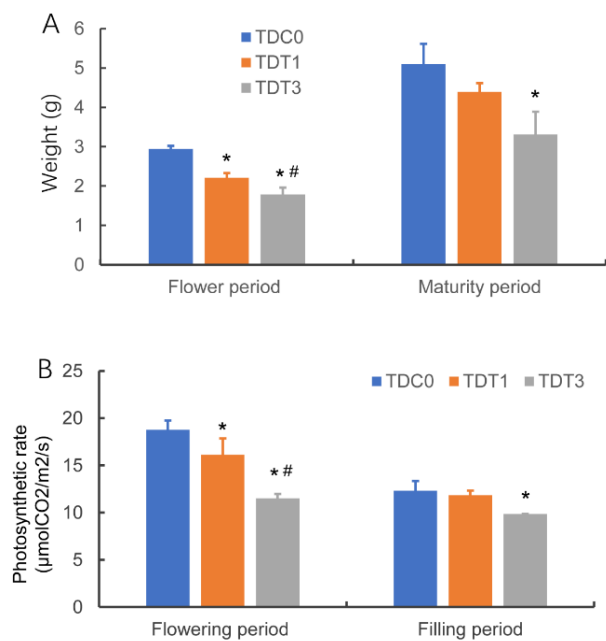
### Hierarchical cluster analysis of DEGs

The FPKM values of DEGs in each group were used for hierarchical clustering analysis. Gene expression patterns were divided into six groups (Fig. 4). Cluster A was enriched with genes showing upregulation in TDT1 and downregulation in TDT3. Cluster B was enriched with genes showing continuous upregulation in TDT1 and TDT3.

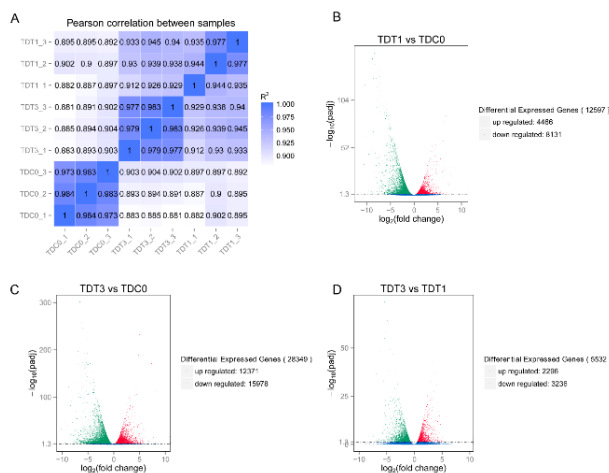
Cluster C was enriched with genes showing downregulation in both TDT1 and TDT3. Cluster D and E were enriched with genes showing downregulation or upregulation only in TDT3. Cluster F was enriched with genes showing downregulation in TDT1 and upregulation in TDT3.

### Functional enrichment of DEGs

The GO enrichment analysis of DEGs between TDT1 and TDC0 as well as between TDT3 and TDC0 were performed. Based on the criteria of corrected  $P$ -value < 0.05, 91 GO terms were significantly enriched by upregulated genes between TDT1 and TDC0, including 29 cellular component (CC) terms, 17 molecular function (MF) terms, and 45 biological process (BP) terms. The GO-BP terms enriched by upregulated genes included cellular homeostasis (Corrected  $P = 9.34e-06$ ,  $n = 50$ ), gene



**Fig. 1:** Changes in the dry weight (A), photosynthetic rate (B) of flag leaves in each group. \*  $P < 0.05$  compared with TDC0; #  $P < 0.05$  compared with TDT1



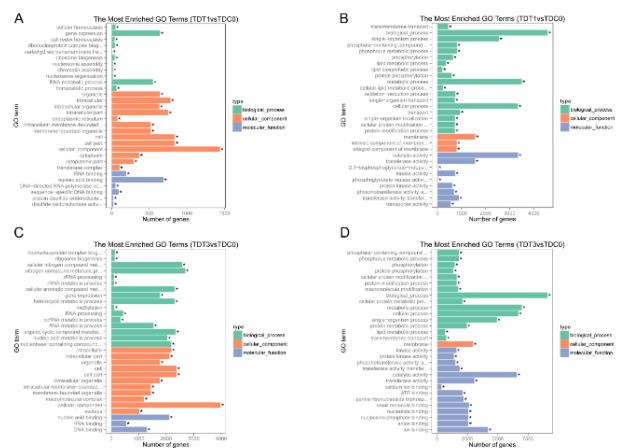


**Fig. 5:** Gene ontology of differentially expressed genes. (A) Gene ontology of the upregulated genes between TDT1, TDC0. (B) Gene ontology of the downregulated genes between TDT1, TDC0. (C) Gene ontology of the upregulated genes between TDT3, TDC0. (D) Gene ontology of the downregulated genes between TDT3, TDC0

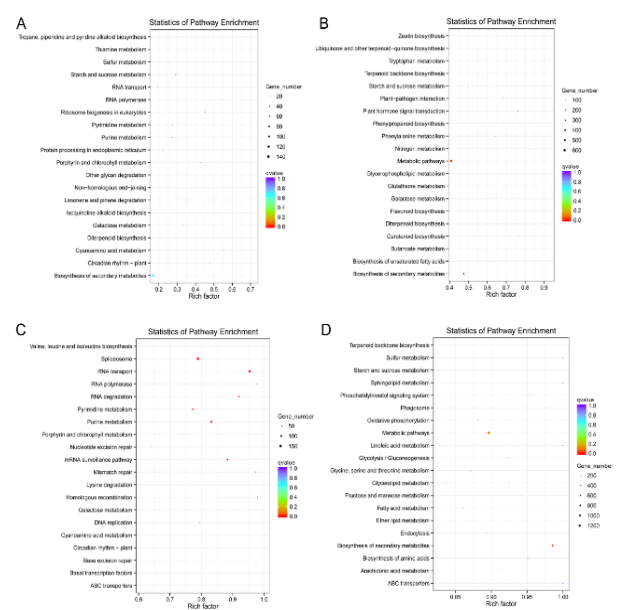


**Fig. 6:** KEGG pathway enrichment analysis of differentially expressed genes. (A) Pathway enrichment analysis of the upregulated genes between TDT1, TDC0. (B) Pathway enrichment analysis of the downregulated genes between TDT1, TDC0. (C) Pathway enrichment analysis of the upregulated genes between TDT3, TDC0. (D) Pathway enrichment analysis of the downregulated genes between TDT3, TDC0

related with protein phosphorylation, including phosphate-containing compound metabolic process (Corrected  $P=2.23e-83$ ,  $n=1,785$ ), phosphorus metabolic process (Corrected  $P=4.26e-83$ ,  $n=1,788$ ), phosphorylation (Corrected  $P=3.09e-81$ ,  $n=1,444$ ), and protein phosphorylation (Corrected  $P=1.18e-75$ ,  $n=1,339$ ) (Fig. 5D).

### KEGG pathway enrichment of DEGs

Based on the criteria of corrected  $P$ -value  $< 0.05$ , seven KEGG terms were significantly enriched by upregulated genes between TDT1 and TDC0, including ribosome biogenesis in eukaryotes (corrected  $P = 1.48e-05$ ,  $n = 41$ ), RNA polymerase (corrected  $P = 0.000291$ ,  $n = 24$ ), cyanoamino acid metabolism (corrected  $P = 0.000957$ ,  $n = 1,444$ ), starch and sucrose metabolism (corrected  $P = 0.0103$ ,  $n = 145$ ), porphyrin and chlorophyll metabolism (corrected  $P = 0.0455$ ,  $n = 35$ ), circadian rhythm – plant (corrected  $P = 0.0463$ ,  $n = 25$ ), and purine metabolism (corrected  $P = 0.0463$ ,  $n = 135$ , Fig. 6A). The downregulated genes between TDT1 and TDC0 were significantly enriched in ten KEGG pathways, including plant hormone signal transduction (corrected  $P = 7.51e-09$ ,  $n = 141$ ), biosynthesis of secondary metabolites (corrected  $P = 0.000217$ ,  $n = 376$ ), plant-pathogen interaction (corrected  $P = 0.000217$ ,  $n = 89$ ), phenylpropanoid biosynthesis (corrected  $P = 0.000217$ ,  $n = 86$ ), phenylalanine metabolism (corrected  $P = 0.00846$ ,  $n = 64$ ), glycerophospholipid metabolism (corrected  $P = 0.0211$ ,  $n = 46$ ), metabolic pathways (corrected  $P = 0.211$ ,  $n = 649$ ), glutathione metabolism (corrected  $P = 0.0246$ ,  $n = 51$ ), nitrogen metabolism (corrected  $P = 0.0363$ ,  $n = 23$ ), and tryptophan metabolism (corrected  $P = 0.0476$ ,  $n = 19$ , Fig. 6B).

Nine KEGG terms were significantly enriched by upregulated genes between TDT3 and TDC0, including RNA transport (corrected  $P = 5.75e-08$ ,  $n = 145$ ), spliceosome (corrected  $P = 3.09e-05$ ,  $n = 156$ ), purine metabolism (corrected  $P = 0.00012$ ,  $n = 113$ ), mRNA surveillance pathway (corrected  $P = 0.00012$ ,  $n = 95$ ), RNA degradation (corrected  $P = 0.00012$ ,  $n = 85$ ), homologous recombination (corrected  $P = 0.00241$ ,  $n = 52$ ), pyrimidine metabolism (corrected  $P = 0.00481$ ,  $n = 87$ ), RNA polymerase (corrected  $P = 0.00712$ ,  $n = 43$ ), and mismatch repair (corrected  $P = 0.00860$ ,  $n = 41$ , Fig. 6C). Only one KEGG pathway term was significantly enriched by downregulated genes between TDT3 and TDC0, which was biosynthesis of secondary metabolites (corrected  $P = 0.004674$ ,  $n = 769$ ; Fig. 6D).

### TFs involved in wheat development

The iTAK software was used to analyze TFs. We identified 2,015 unigenes as TFs. The main TF families identified were MYB (134 unigenes), WRKY (126 unigenes), AP2-EREBP (120 unigenes), bHLH (112 unigenes), NAC (112 unigenes), bZIP (86 unigenes), and FAR1 (83 unigenes) (Table 3).

### The qRT-PCR validation of genes involved in photosynthesis

Since the RNA-Seq data were high-throughput and might generate some false-discovery results, we used qRT-PCR to validate some important genes in response to shading

**Table 3:** Number of unigenes in each transcription factor family

Family	Number
MYB	134
WRKY	126
AP2-EREBP	120
bHLH	112
NAC	112
bZIP	86
Orphans	84
FAR1	83
HB	69
C2H2	60
mTERF	57
C3H	56
G2-like	52
GRAS	46
AUX/IAA	43
HSF	41
AB13VP1	40
SET	39
SNF2	36
C2C2-Dof	35
PHD	33
CCAAT	31
C2C2-GATA	30
GNAT	30
ARF	29
MADS	28
Tify	27
TUB	25
TRAF	23

**Table 4:** Gene expression changes of the seven genes in TDT1 versus TDC0, TDT3 versus TDC0 in RNA-seq results

Gene	log2FoldChange (TDT1 vs TDC0)	log2FoldChange (TDT3vs TDC0)
CYP98A1	-2.8049	-3.5722
At3g21620	-2.3869	-2.0606
ACO1	-6.3004	-5.1099
ETR1	-2.2315	-2.0732
1-SST	-3.7623	-4.4975
PSB28	-2.8358	-2.8358
HEMH	-0.79888	-1.2236
WHAB1.6	-1.101	-2.9141
Os10g0493600	1.2544	1.0797
6-FEH	0.67194	2.3548
CIN2	1.4464	3.4538
PORA	2.1397	5.1143
At5g26707	2.1447	2.2296
CPX	0.83205	1.70035
PPO	2.0957	2.4764
PKL	1.1797	1.9068

treatment. Sixteen DEGs involved in porphyrin and chlorophyll metabolism, photosynthesis, and galactose metabolism were selected to be validated, including eight downregulated genes of *CYP98A1*, *At3g21620*, *ACO1*, *ETR1*, *1-SST*, *PSB28*, *HEMH*, and *WHAB1.6*; and eight upregulated genes of *Os10g0493600*, *6-FEH*, *CIN2*, *PORA*, *At5g26707*, *CPX*, *PPO*, and *PKL* (Table 4). Five of the eight downregulated genes (*At3g21620*, *ETR1*, *1-SST*, *PSB28*, and *HEMH*) and five of the eight upregulated genes (*Os10g0493600*, *6-FEH*, *CIN2*, *PORA*, and *CPX*) were successfully validated by qRT-PCR, indicating these genes may play important roles in shading conditions (Fig. 7).

## Discussion

In the present study, we sequenced transcriptomes of leaves under different shading levels using Next Generation RNA-seq to comprehensively characterize gene changes under different shading levels. A total of 12,597 DEGs were identified between TDT1 and TDC0, and a total of 28,349 DEGs were identified between TDT3 and TDC0. In this study, the hierarchical cluster analysis showed that these DEGs can be divided into six clusters with different gene expression patterns. Functional results showed that the upregulated genes between TDT1 and TDC0 were significantly enriched into cellular homeostasis and cell redox homeostasis, and those between TDT3 and TDC0 were significantly enriched into cellular nitrogen compound metabolic process and nitrogen compound metabolic process. From this study, the downregulated genes between TDT1 and TDC0 as well as those between TDT3 and TDC0 were both significantly enriched in phosphorus metabolic processes, such as phosphorus metabolic process, protein phosphorylation, phosphate-containing compound metabolic process and phosphorylation.

Cell homeostasis, especially redox homeostasis, is important for the maintenance of many cellular processes, including the removal of xenobiotics, protection of protein thiols, maintenance of oxidation-reduction balance, and response to reactive oxygen species (ROS) (Ayer *et al.* 2014). Plant cell redox homeostasis is formed as a result of the balance between ROS and antioxidant interaction, and it acts as a metabolic interface for signals derived from metabolism and environment (Foyer and Noctor 2005). We assume that shading stress triggers specific networks of biological processes involved in redox and ionic homeostasis. According to this study, tens genes involved in redox homeostasis were upregulated, including several genes encoding redoxins (*GRXC1*, *GRXC14*, and *GLRX2*), glutathione S-transferase U10 (*GSTU10*), and thioredoxin-like proteins (*TRL11*, *TRL31*, *CXXS1*, *CDSP32*, *CITRX*, *YLS8*, and *WCRKC2*). Glutaredoxin is a small redox enzyme, which is an indispensable element of the plant antioxidant system to keep proteins in their properly reduced states (Rouhier *et al.* 2006; Meyer *et al.* 2012). Glutaredoxins were reported to be activated under several abiotic stresses, such as oxidative stress and drought (Kanda *et al.* 2006; Ding *et al.* 2019). Usually, a massive ROS was accumulated in plants when they suffer from abiotic stresses, and the activation of glutaredoxins could prevent plants from damage by scavenging ROS (Hasanuzzaman *et al.* 2013). *GSTU10* is a member of the Tau family of glutathione S-transferases (GSTs), which are plant-specific and can bind glutathione conjugated fatty acid derivatives (Dixon and Edwards 2009). In a previous study, the upregulation of *GSTU10* was also found in *Arabidopsis* with inducible nicotinamide adenine dinucleotide (NAD) overproduction (Petriacq *et al.* 2012) and in *Arabidopsis* infected with *Botrytis cinerea* (Windram *et al.* 2012).

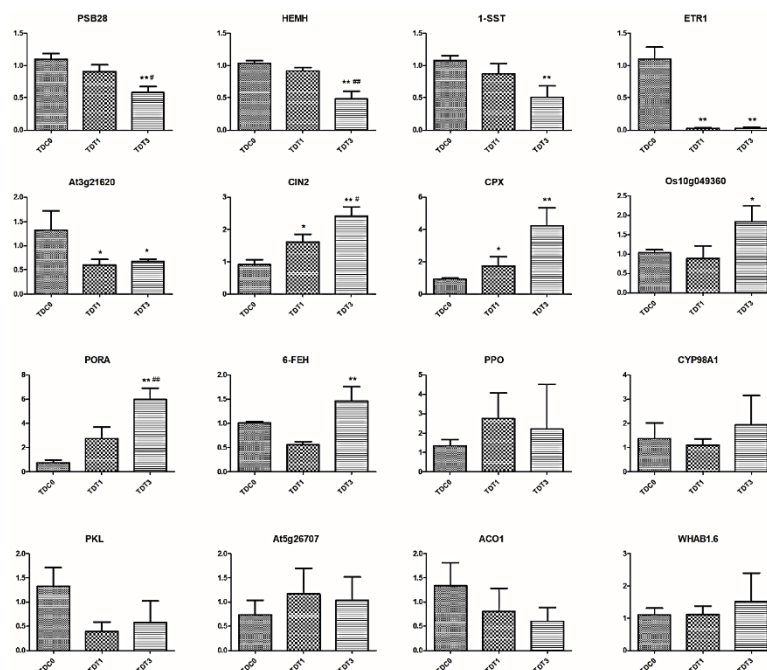


**Fig. 7:** Validation of 16 genes by qRT-PCR. \*  $P < 0.05$  compared with TDC0; \*\*  $P < 0.01$  compared with TDC0; #  $P < 0.05$  compared with TDT1; ##  $P < 0.01$  compared with TDT1

Thioredoxin-like proteins are homologous with thioredoxins which was characterized by the presence of six tetratricopeptide repeats in conserved positions (Lakhssassi *et al.* 2012). Several members of thioredoxin-like proteins were reported to be involved in abiotic stress tolerance, such as *TTL1*, *TTL3*, and *TTL4* (Borsani *et al.* 2002; Rosado *et al.* 2006; Lakhssassi *et al.* 2012). Since *Arabidopsis* *TTL1* is functioned in osmotic stress tolerance, a large-scale upregulation of thioredoxin-like proteins in this study suggests that these proteins may be important for appropriate responses to shade stress. Generally, wheat development under 25% shading is adaptively modulated by a steady-state balance between ROS and phytohormones.

In this study, in 75% shading group, the upregulated genes were significantly enriched in nitrogen compound metabolic process and the downregulated genes were significantly enriched in phosphorus metabolic processes. Nitrogen and phosphorus are essential elements in plant growth and they have many roles in photosynthetic organisms. Plants well-supplemented with nitrogen can produce higher levels of photosynthetic pigments, and this allows higher electron transport rates in chloroplasts (Evans and Poorter 2001). However, under shading, nitrogen allocation is destined to greater chlorophyll biosynthesis in light-harvesting systems (Hikosaka and Terashima 1995; 1996; Valladares and Niinemets 2008). This might lead to structural and physiological changes in plants to acclimatize low irradiance conditions, such as architectural modifications both in stems and leaves to increase leaf area (Falcioni *et al.* 2018). These changes tend to reduce the maximum photosynthetic leaf area capacity, but increase

mass-basis photosynthesis (Percy *et al.* 2005). Therefore, we speculated that wheat survival under shading might result in the allocation of nitrogen and phosphorus to acclimatize to low irradiance conditions.

TFs regulate gene transcriptions. This study showed that several TFs, including MYB, WRKY, AP2-EREBP, bHLH, and bZIP family members, were differentially expressed. bZIP TFs are essential in regulating light and stress signaling, pathogen defense, flower development and seed maturation (Jakoby *et al.* 2002). Chang *et al.* (2019) identified CaLMF as a significant light signaling component mediating light-regulated camptothecin biosynthesis under shading treatment. WRKYs are also widely involved in plant responses to biotic and abiotic stress (Zhu *et al.* 2013). Similarly, the MYB gene family plays an important role in regulatory networks that control development, metabolism and environmental stresses response (Dubos *et al.* 2010). Wang *et al.* (2015) demonstrated that eight MYB genes were apparently induced, and three genes were repressed under shading treatment.

## Conclusion

This study characterized the transcriptome profile of wheat in response to different shading levels. A total of 12,597 and 28,349 DEGs were identified in 25 and 75% shading groups, respectively, compared with the control. Functional enrichment analyses suggested that the upregulated genes in 25% shading group were mainly involved in regulating cell homeostasis, especially in redox homeostasis. The upregulated genes in 75% shading group were involved in

nitrogen compound metabolic process and the downregulated genes of the two groups were both enriched in phosphorus metabolic processes. Ten of the 16 DEGs involved in porphyrin and chlorophyll metabolism, photosynthesis, and galactose metabolism were successfully validated by qRT-PCR. These data provided detailed transcriptional changes of wheat in response to different shading levels and contribute to systemically explained gene regulatory networks mediating the wheat response to shading.

## Acknowledgement

This work was financially supported by the National Key Research and Development Program of China (No. 2016YFD0300110) and the National Natural Science Foundation of China (No. 31560370).

## Author's contribution

Qi Zhao conceived and designed the experiments; Xiaorong Li and Jianfeng Li performed the experiments and wrote the paper; Hongzhi Zhang and Lihong Wang performed the field experiments; Zhong Wang, Yueqiang Zhang and Jia Shi analyzed the data; Zheru Fan contributed materials for use in the experiments.

## References

- Anders S, P T Pyl, W Huber (2015). HTSeq—a Python framework to work with high-throughput sequencing data. *Bioinformatics* 31:166–169
- Ashburner M, CA Ball, JA Blake, D Botstein, HL Butler, JM Cherry, AP Davis, K Dolinski, SS Dwight, JT Eppig, MA Harris, DP Hill, L Isseltarver, A Kasarskis, SE Lewis, JC Matese, JE Richardson, M Ringwald, GM Rubin, G Sherlock (2000). Gene ontology: Tool for the unification of biology. *Nat Genet* 25:25–29
- Ayer A, CW Gourlay, IW Dawes (2014). Cellular redox homeostasis, reactive oxygen species, replicative ageing in *Saccharomyces cerevisiae*. *FEMS Yeast Res* 14:60–72
- Batool S, A Wahid, SMA Basra, M Shahbaz (2020). Light augments the action of foliar applied plant growth regulators: Evidence using etiolated maize (*Zea mays*) seedlings. *Intl J Agric Biol* 23:801–810
- Benjamini Y, Y Hochberg (1995). Controlling the false discovery rate: A practical, powerful approach to multiple testing. *J Royal Stat Soc Ser B (Methodological)* 57:289–300
- Bergeron M, S Lacombe, RL Bradley, J Whalen, A Cogliastro, MF Jutras, P Arp (2011). Reduced soil nutrient leaching following the establishment of tree-based intercropping systems in eastern Canada. *Agrofor Syst* 83:321–330
- Borsani O, J Cuartero, V Valpuesta, MA Botella (2002). Tomato *tos1* mutation identifies a gene essential for osmotic tolerance, abscisic acid sensitivity. *Plant J* 32:905–914
- Carbon S, J Chan, R Kishore, R Lee, HM Muller, D Raciti, KV Auken, PW Sternberg (2017). Expansion of the Gene Ontology knowledgebase, resources. *Nucl Acids Res* 45:D331–D338
- Chang CH, ZW Liu, YY Wang, ZH Tang, F Yu (2019). A bZIP transcription factor, CaLMF, mediated light-regulated camptothecin biosynthesis in *Camptotheca acuminata*. *Tree Physiol* 39:372–380
- Cossani CM, MP Reynolds (2012). Physiological traits for improving heat tolerance in wheat. *Plant Physiol* 160:1710–1718
- Ding SC, FY He, WL Tang, HW Du, HW Wang (2019). Identification of maize CC-type glutaredoxins that are associated with response to drought stress. *Genes Basel* 10; Article 610
- Dixon DP, R Edwards (2009). Selective binding of glutathione conjugates of fatty acid derivatives by plant glutathione transferases. *J Biol Chem* 284:21249–21256
- Dubos C, R Stracke, E Grotewold, B Weisshaar, C Martin, L Lepiniec (2010). MYB transcription factors in Arabidopsis. *Trends Plant Sci* 15:573–581
- Evans JR, H Poorter (2001). Photosynthetic acclimation of plants to growth irradiance: the relative importance of specific leaf area, nitrogen partitioning in maximizing carbon gain. *Plant Cell Environ* 24:755–767
- Falcioni R, T Moriwaki, E Benedito, CM Bonato, LA de Souza, WC Antunes (2018). Increased gibberellin levels enhance the performance of light capture efficiency in tobacco plants, promote dry matter accumulation. *Exp Plant Physiol* 30:235–250
- Foyer CH, G Noctor (2005). Redox homeostasis, antioxidant signaling: a metabolic interface between stress perception, physiological responses. *Plant Cell* 17:1866–1875
- Gao JW, QC Luo, CJ Sun, H Hu, F Wang, ZW Tian, D Jiang, WW Cao, TB Dai (2019). Low nitrogen priming enhances photosynthesis adaptation to water-deficit stress in winter wheat (*Triticum aestivum* L.) Seedlings. *Front Plant Sci* 10; Article 818
- Guo Z, Z Yu, D Wang, Y Shi, Y Zhang (2014). Photosynthesis, winter wheat yield responses to supplemental irrigation based on measurement of water content in various soil layers. *Field Crops Res* 166:102–111
- Hasanuzzaman M, K Nahar, MM Alam, R Roychowdhury, M Fujita (2013). Physiological, biochemical, molecular mechanisms of heat stress tolerance in plants. *Intl J Mol Sci* 14:9643–9684
- Hikosaka K, I Terashima (1995). A model of the acclimation of photosynthesis in the leaves of C3 plants to sun, shade with respect to nitrogen use. *Plant Cell Environ* 18:605–618
- Hikosaka K, I Terashima (1996). Nitrogen partitioning among photosynthetic components, its consequences in sun, shade plants. *Funct Ecol* 10:335–343
- Jakoby M, B Weisshaar, W Dröge-Laser, J Vicente-Carbajosa, J Tiedemann, T Kroj, F Parcy (2002). bZIP transcription factors in Arabidopsis. *Trends Plant Sci* 7:106–111
- Kanda M, Y Ihara, H Murata, Y Urata, T Kono, J Yodoi, S Seto, K Yano, T Kondo (2006). Glutaredoxin modulates platelet-derived growth factor-dependent cell signaling by regulating the redox status of low molecular weight protein-tyrosine phosphatase. *J Biol Chem* 281:28518–28528
- Kemp D, E Whingwiri (1980). Effect of tiller removal, shading on spikelet development, yield components of the main shoot of wheat, on the sugar concentration of the ear, flag leaf. *Aust J Plant Physiol* 7:501–510
- Kim D, B Langmead, SL Salzberg (2015). HISAT: A fast spliced aligner with low memory requirements. *Nat Methods* 12:357–360
- Lakhssassi N, VG Doblaz, A Rosado, AE Del Valle, D Pose, AJ Jimenez, AG Castillo, V Valpuesta, O Borsani, MA Botella (2012). The Arabidopsis tetratricopeptide thioredoxin-like gene family is required for osmotic stress tolerance, in male sporogenesis. *Plant Physiol* 158:1252–1266
- Li HW, D Jiang, B Wollenweber, TB Dai, WW Cao (2010). Effects of shading on morphology, physiology, grain yield of winter wheat. *Eur J Agron* 33:267–275
- Li Q, SF Zhong, SF Sun, SA Fatima, M Zhang, WQ Chen, QL Huang, SW Tang, PG Luo (2017). Differential effect of whole-ear shading after heading on the physiology, biochemistry, yield index of stay-green, non-stay-green wheat genotypes. *PLoS One* 12:Article e0171589
- Livak J, TD Schmittgen (2001). Analysis of relative gene expression data using real-time quantitative PCR, the 2(-Delta Delta C(T)) method. *Methods* 25:402–408
- Love MI, W Huber, S Anders (2014). Moderated estimation of fold change, dispersion for RNA-seq data with DESeq2. *Genome Biol* 15; Article 550
- Makino A (2011). Photosynthesis, grain yield, nitrogen utilization in rice, wheat. *Plant Physiol* 155:125–129

- Mao XZ, T Cai, JG Olyarchuk, LP Wei (2005). Automated genome annotation, pathway identification using the KEGG Orthology (KO) as a controlled vocabulary. *Bioinformatics* 21:3787–3793
- Meyer Y, C Belin, V Delormehinoux, J Reichheld, C Riondet (2012). Thioredoxin, glutaredoxin systems in plants: molecular mechanisms, crosstalks, functional significance. *Antioxid Redox Signal* 17:1124–1160
- Mu H, D Jiang, B Wollenweber, TB Dai, QJing, WW Cao (2010). Long-term low radiation decreases leaf photosynthesis, photochemical efficiency, grain yield in winter wheat. *J Agron Crop Sci* 196:38–47
- Pearcy RW, H Muraoka, F Valladares (2005). Crown architecture in sun, shade environments: assessing function, trade-offs with a three-dimensional simulation model. *New Phytol* 166:791–800
- Petriaq P, LD Bont, J Hager, L Didierlaurent, C Mauve, F Guerard, G Noctor, S Pelletier, J Renou, G Tcherkez, B Gakiere (2012). Inducible NAD overproduction in Arabidopsis alters metabolic pools, gene expression correlated with increased salicylate content, resistance to Pst-AvrRpm1. *Plant J* 70:650–65
- Qiao X, LH Sai, X Chen, LH Xue, JJ Lei (2019). Impact of fruit-tree shade intensity on the growth, yield, quality of intercropped wheat. *PLoS One* 14; Article e0203238
- Rivest D, M Lorente, A Olivier, C Messier, (2013). Soil biochemical properties, microbial resilience in agroforestry systems: Effects on wheat growth under controlled drought, flooding conditions. *Sci Total Environ* 463–464:51–60
- Rivest D, A Cogliaastro, A Olivier (2009). Tree-based intercropping systems increase growth, nutrient status of hybrid poplar: A case study from two Northeastern American experiments. *J Environ Manage* 91:432–440
- Rosado A, AL Schapiro, RA Bressan, AL Harfouche, PM Hasegawa, V Valpuesta, MA Botella (2006). The Arabidopsis tetratricopeptide repeat-containing protein TTL1 is required for osmotic stress responses, abscisic acid sensitivity. *Plant Physiol* 142:1113–1126
- Rouhier N, J Couturier, J Jacquot (2006). Genome-wide analysis of plant glutaredoxin systems. *J Exp Bot* 57:1685–1696
- Trapnell C, BA Williams, G Pertea, A Mortazavi, G Kwan, MJV Baren, SL Salzberg, BJ Wold, L Pachter (2010). Transcript assembly, quantification by RNA-Seq reveals unannotated transcripts, isoform switching during cell differentiation. *Nat Biotechnol* 28:511–515
- Valladares F, U Niinemets (2008). Shade tolerance, a key plant feature of complex nature, consequences. *Annu Rev Ecol Evol Syst* 39:237–257
- Wang FQ, YF Suo, H Wei, MJ Li, CX Xie, LN Wang, XJ Chen, ZY Zhang (2015). Identification, characterization of 40 isolated *Rehmannia glutinosa* MYB family genes, their expression profiles in response to shading, continuous cropping. *Intl J Mol Sci* 16:15009–15030
- Wang Z, Y Yin, M He, Y Zhang, S Lu, Q Li, S Shi (2003). Allocation of photosynthates, grain growth of two wheat cultivars with different potential grain growth in response to pre-, post-anthesis shading. *J Agron Crop Sci* 189:280–285
- Windram OP, P Madhou, S Mchattie, C Hill, R Hickman, EJ Cooke, DJ Jenkins, CA Penfold, L Baxter, E Breeze, SJ Kiddle, J Rhodes, S Atwell, DJ Kliebenstein, Y Kim, O Stegle, KM Borgwardt, C Zhang, A Tabrett, R Legaie, JD Moore, B Finkenstadt, DL Wild, A Mead, DA Rand, J Beynon, S Ott, V Buchananwollaston, KJ Denby (2012). Arabidopsis defense against *Botrytis cinerea*: Chronology, regulation deciphered by high-resolution temporal transcriptomic analysis. *Plant Cell* 24:3530–3557
- Wu HY, NR Shi, XY An, C Liu, HF Fu, L Cao, Y Feng, DJ Sun, LL Zhang (2018). Candidate genes for yellow leaf color in common wheat (*Triticum aestivum* L.), major related metabolic pathways according to transcriptome profiling. *Intl J Mol Sci* 19; Article e1594
- Xu CL, HB Tao, P Wang, ZL Wang (2016). Slight shading after anthesis increases photosynthetic productivity, grain yield of winter wheat (*Triticum aestivum* L.) due to the delaying of leaf senescence. *J Integr Agric* 15:63–75
- Young MD, MJ Wakefield, GK Smyth, A Oshlack (2010). Gene ontology analysis for RNA-seq: accounting for selection bias. *Genome Biol* 11; Article R14
- Yu Y, TJ Stomph, D Makowski, Wd Werf (2015). Temporal niche differentiation increases the land equivalent ratio of annual intercrops: A meta-analysis. *Field Crops Res* 184:133–144
- Zheng Y, C Jiao, HH Sun, HG Rosli, MA Pombo, PF Zhang, M Banf, XB Dai, GB Martin, JJ Giovannoni, PX Zhao, SY Rhee, ZJ Fei (2016). iTAK: A program for genome-wide prediction, classification of plant transcription factors, transcriptional regulators, protein kinases. *Mol Plant* 9:1667–1670
- Zhu XL, SW Liu, C Meng, LM Qin, LN Kong, GM Xia (2013). *WRKY* transcription factors in wheat, their induction by biotic, abiotic stress. *Plant Mol Biol Rep* 31:1053–1067